BIOCHEMISTRY
including biophysical chemistry & molecular biology

Accelerated Publication

pubs.acs.org/biochemistry

# Structure of EvaA: A Paradigm for Sugar 2,3-Dehydratases

Rachel L. Kubiak, James B. Thoden, and Hazel M. Holden*

Department of Biochemistry, University of Wisconsin, Madison, Wisconsin 53706, United States

Supporting Information

**ABSTRACT:** Unusual deoxysugars found appended to natural products often provide or enhance the pharmacokinetic activities of the parent compound. The preferred carbohydrate donors for the biosynthesis of such glycosylated natural products are the dTDP-linked sugars. Many of the biologically relevant dTDP-deoxysugars are constructed around the 2,6-dideoxyhexoses or the 2,3(4),6-trideoxyhexoses. A key step in the biosynthesis of these sugars is the removal of the hexose C-2′ hydroxyl group and the oxidation of the C-3′ hydroxyl group to a carbonyl moiety. Enzymes that catalyze these reactions are referred to as 2,3-dehydratases and have been, for the most part, largely uncharacterized. Here we report the first structural analysis of a sugar 2,3-dehydratase. For this investigation, the enzyme, EvaA, was cloned from *Amycolatopsis orientalis*, and the structure was solved and refined to a nominal resolution of 1.7 Å. On the basis of the resulting model, it is clear that EvaA belongs to the large Nudix hydrolase superfamily and is most similar to GDP-mannose hydrolase. Each subunit of the EvaA dimer folds into two domains that clearly arose via gene duplication. Two dTDP-sugar binding pockets, A and B, are present in each EvaA subunit. On the basis of site-directed mutagenesis experiments and activity assays, it appears that pocket A functions as the active site and pocket B is simply a remnant left behind from the gene duplication event. As 2,3-dehydration is crucial for the biosynthesis of many unusual deoxysugars, this investigation provides key structural insight into this widely conserved reaction.

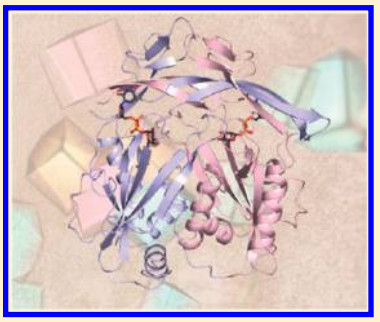

Recent years have witnessed an explosion in research efforts directed at uncovering and understanding the biosynthesis of unusual di- and trideoxysugars.[1,2] These intriguing carbohydrates are synthesized by a variety of bacteria, fungi, and plants and are observed, for example, on the lipopolysaccharides of some Gram-negative bacteria or on antibacterial, antitumor, and/or antifungal agents. One such sugar is L-epivancosamine, a 2,3,6-trideoxysugar found appended to the aglycone scaffold of the antibiotic chloroeremomycin.[3] Interestingly, chloroeremomycin has been shown to be a more potent antibiotic than vancomycin, presumably because of the presence of L-epivancosamine.[4] Indeed, the di- and trideoxysugars are often critical for the efficacies of the compounds to which they are attached.[5]

As indicated in Scheme 1, five enzymes are required for the production of dTDP-epivancosamine.[6] The focus of this study is EvaA from *Amycolatopsis orientalis*, a 2,3-dehydratase that catalyzes the first step in the pathway, namely the removal of the hydroxyl group at position C-2′ of the hexose ring and the oxidation of the hydroxyl group at position C-3′ to a carbonyl functionality. The product of the EvaA reaction is a highly unstable diketosugar. Other than an initial characterization of the enzyme, little is known with regard to its structure or catalytic mechanism.[6] A homologous enzyme from *Streptomyces fradiae*, TylX3, has been partially characterized, however.[7] It has been shown to function as a dimer and reportedly requires zinc for activity. Several functions for the zinc ion have been postulated. (i) It acts as a catalytic base by activating a water molecule. (ii) It is responsible for polarizing the C-4′ keto group of the sugar substrate to facilitate the generation of an enolate species. (iii) It serves as an active site Lewis acid to aid in the departure of the 2′-hydroxyl group.[8]

Amino acid sequence alignments demonstrate that both EvaA and TylX3 exhibit a high degree of similarity to other 2,3-dehydratases (~50% identical and ~70% similar) involved in the production of antibiotics and antitumor agents, including those found in the biosynthetic pathways for erythromycin, landomycin, nogalamycin, doxorubicin, and granaticin, among others.[9−12] Importantly, however, searches of the amino acid sequences for these enzymes against known structures in the Protein Data Bank have provided no clues about the overall fold of any sugar 2,3-dehydratase.

Here we report the first high-resolution structure of a sugar 2,3-dehydratase (EvaA) determined to 1.7 Å resolution and crystallized in the presence of a substrate analogue. Each subunit of the dimer folds into two domains, which are related by a 2-fold rotational axis and which clearly arose via gene duplication. The overall molecular architecture places EvaA into the well-characterized "Nudix" hydrolase family, members of which often function as "housekeeping" enzymes.[13,14] Two binding sites for the dTDP-sugar ligands, pockets A and B, have been identified in each subunit. Site-directed mutagenesis experiments and activity assays strongly suggest that pocket A represents the active site and pocket B is a vestige of the gene duplication event. Strikingly, no zinc ions were observed in the electron density maps, and there are no apparent zinc-binding

**Received:** February 12, 2013
**Revised:** March 7, 2013
**Published:** March 8, 2013

  

**Scheme 1. dTDP-Epivancosamine Biosynthetic Pathway**

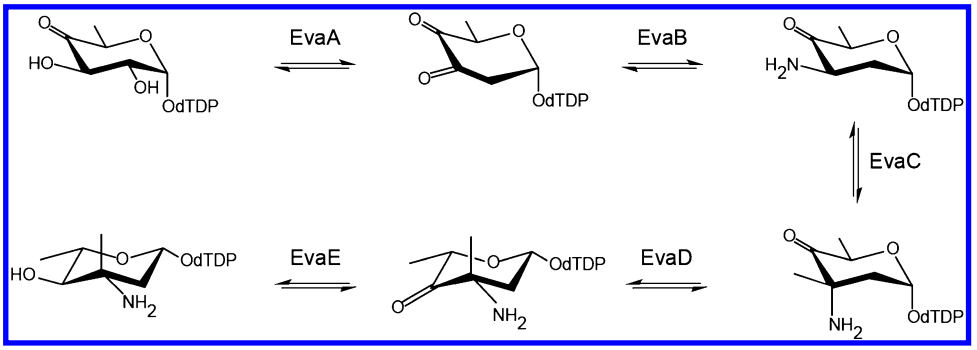


**Table 1. X-ray Data Collection Statistics**

| | crystals of the selenomethionine-labeled protein | crystals of the enzyme in a complex with dTDP-fucose | crystals of the enzyme soaked in dTDP-benzene |
|---|---|---|---|
| resolution limits (Å) | 50.0−3.62 (3.62−3.48)[b] | 50.0−1.70 (1.86−1.70)[b] | 50.0−1.70 (1.86−1.70)[b] |
| no. of independent reflections | 33398 (3692) | 133160 (12674) | 135159 (12455) |
| completeness (%) | 99.5 (99.5) | 95.7 (92.0) | 97.2 (90.7) |
| redundancy | 4.7 (4.7) | 6.1 (3.2) | 7.0 (3.5) |
| avg $I$/avg $\sigma(I)$ | 35.9 (10.5) | 40.2 (3.6) | 55.7 (6.3) |
| $R_{sym}$ (%)[a] | 9.9 (19.9) | 8.1 (26.6) | 5.4 (14.5) |

[a] $R_{sym} = (\sum|\sum I - \overline{I}|/\sum I) \times 100$. [b] Statistics for the highest-resolution bin.

motifs. Taken together, the results of this investigation provide a molecular foundation for understanding the sugar 2,3-dehydratases, whose structures have remained elusive until now.

## MATERIALS AND METHODS

**Cloning, Expression, and Purification.** The gene encoding EvaA was amplified from *A. orientalis* NRRL18098 by standard polymerase chain reaction methods and ultimately ligated into a pET28JT vector for protein production with a TEV protease-cleavable N-terminal hexahistidine tag.[15] The pET28JT-EvaA plasmid was used to transform Rosetta2(DE3) *Escherichia coli* cells (Novagen). Cultures were grown while being shaken in lysogeny broth supplemented with kanamycin at 37 °C until optical densities of 0.8 were reached at 600 nm. The flasks were then cooled to 16 °C, and the cells were subsequently induced with the addition of 1 mM isopropyl β-D-1-thiogalactopyranoside. These cells were allowed to express protein at 16 °C for 18 h.

EvaA was purified by standard procedures using Ni-nitrilotriacetic resin (Qiagen). Purified protein was dialyzed against 25 mM HEPES (pH 7.5) and 100 mM NaCl, concentrated to ∼25 mg/mL, and flash-frozen in liquid nitrogen. For production of protein with the His tag removed, the purified enzyme was incubated in the presence of 1 mM DTT and TEV protease at a 50:1 EvaA:TEV protease molar ratio at 4 °C for 36 h. The TEV protease was subsequently removed via Ni-nitrilotriacetic acid column chromatography. The untagged version of EvaA was then dialyzed and frozen in the same manner as described above.

**Structural Analysis of EvaA.** Crystallization conditions were initially surveyed at room temperature via the hanging drop method of vapor diffusion using a sparse matrix screen developed in the laboratory. Crystals of the N-terminally His-tagged protein at a concentration of 25 mg/mL with 10 mM dTDP-fucose (dTDP-6-deoxygalactose) were grown by mixing in a 1:1 ratio the enzyme solution with 1.0−1.1 M ammonium sulfate and 100 mM MES (pH 5.5). Production of the required dTDP-fucose ligand is described below. The EvaA crystals belonged to the space group $P2_1$ with four monomers in the asymmetric unit and the following unit cell dimensions: $a$ = 105.2 Å, $b$ = 113.3 Å, $c$ = 110.9 Å, and $\beta$ = 98.8°. For phasing purposes, a selenomethionine-labeled version of the protein was prepared and crystallized in the same manner.

X-ray data sets from crystals of both the wild-type and the selenomethionine-labeled proteins were collected at the Structural Biology Center Beamline 19-BM at wavelengths of 0.980 Å (peak) and 0.98019 Å (inflection) (Advanced Photon Source, Argonne National Laboratory, Argonne, IL). The data were processed and scaled with HKL3000.[16] X-ray data collection statistics are listed in Table 1. Twenty-two selenium sites were located using SOLVE, yielding a figure of merit of 0.32 to 3.5 Å resolution.[17] A preliminary model was constructed with COOT.[18] Unfortunately, the map was not of sufficient quality to unambiguously trace the polypeptide chain backbone, although approximately two-thirds of the side chains could be identified.

Given the poor quality of the electron density map, it became clear that higher-order crystals would be necessary to complete the structural analysis of EvaA. With that in mind, various site-directed mutant proteins were constructed. Specifically, four proteins with single mutations, two proteins with double mutations, and one protein with a triple mutation were produced. The four proteins with single mutations were selected for study because of their positions on the surface of the EvaA model. It was hypothesized that changing these residues, Asp 127, Arg 381, Asp 386, and Ser 394, might influence crystal packing and reduce the contents of the asymmetric unit. All four residues were changed to alanines. The two proteins with double mutations (E231A/E233A and E316A/E317A) and the one protein with a triple mutation


dx.doi.org/10.1021/bi400176n | *Biochemistry* 2013, 52, 2078−2088

(K289A/Q290A/E293A) were chosen for study on the basis of suggestions from the surface entropy reduction server.[19,20]

The mutations were introduced via methods identical or similar to those described within the QuikChange site-directed mutagenesis kit (Stratagene). All primers used in this investigation are listed in Table S1 of the Supporting Information. The cloning procedures were conducted with the pET28JT-*EvaA* plasmid. Each mutant protein was expressed and purified in a manner identical to that previously described for the wild-type protein except that the mutant proteins were dialyzed against 10 mM Tris (pH 8.0) and 200 mM NaCl and concentrated to 13−18 mg/mL.

Crystallization conditions were screened at room temperature for all 14 mutant proteins via the hanging drop method of vapor diffusion. X-ray diffraction-quality crystals of the TEV-cleaved R381A single mutant protein were obtained by mixing in a 1:1 ratio of the protein solution (14 mg/mL with 5 mM dTDP-fucose) and a solution containing 20% poly(ethylene glycol) 8000 and 100 mM HEPES (pH 7.5). These crystals belonged to the space group $P2_12_12$ with two rather than four subunits in the asymmetric unit and the following unit cell dimensions: $a$ = 105.8 Å, $b$ = 108.2 Å, and $c$ = 110.2 Å. Importantly, these crystals diffracted to a nominal resolution of 1.7 Å.

Prior to X-ray data collection, single crystals of the EvaA R381A−dTDP-fucose complex were transferred to a synthetic mother liquor containing 21% poly(ethylene glycol) 8000, 200 mM NaCl, 5 mM dTDP-fucose, and 100 mM HEPES (pH 7.5). Subsequently, these crystals were transferred in five steps to a cryoprotectant solution containing 23% poly(ethylene glycol) 8000, 200 mM NaCl, 5 mM dTDP-fucose, 15% ethylene glycol, and 100 mM HEPES (pH 7.5).

A high-resolution X-ray data set was collected at the Structural Biology Center Beamline 19-ID at a wavelength of 0.979 Å (Advanced Photon Source). The data were processed and scaled with HKL3000.[16] The higher-resolution structure of EvaA was determined via molecular replacement with Phaser and using as a search model the low-resolution EvaA monomer that had been previously built.[21] The resulting map was further improved by molecular averaging with DM.[22] Iterative rounds of refinement with Refmac and manual model building with COOT led to a final overall $R$ factor of 17.3% for all measured X-ray data from 50 to 1.7 Å resolution.[23] Relevant X-ray data collection and refinement statistics are listed in Tables 1 and 2, respectively.

As the high-resolution model of EvaA R381A was being built, it became clear that the enzyme had two dTDP-sugar binding pockets per subunit. One of the binding pockets was clearly the functional active site, whereas the other was a "leftover" from the gene duplication event that apparently occurred during the evolution of EvaA. To test which binding pocket might exchange the ligand more easily, crystals of the EvaA R381A−dTDP-fucose complex were soaked in a synthetic mother liquor containing 20 mM dTDP-benzene rather than dTDP-fucose and flash-cooled.

An X-ray data set from a dTDP-benzene-soaked crystal was collected to 1.7 Å resolution and processed as described for the EvaA R381A−dTDP-fucose complex. The structure of the ligand-exchanged enzyme was determined by molecular replacement with Phaser using the EvaA R381A high-resolution structure as a search model with the dTDP-sugar ligands removed. The model was rebuilt with Coot and refined with Refmac. Relevant X-ray data collections and refinement statistics are listed in Tables 1 and 2, respectively.

**Table 2. Refinement Statistics**

| | crystals of the enzyme in a complex with dTDP-fucose | crystals of the enzyme soaked in dTDP-benzene |
|---|---|---|
| resolution limits (Å) | 50.0−1.70 | 50.0−1.70 |
| $R$ factor (overall) (%)/no. of reflections[a] | 17.3/133122 | 16.6/135133 |
| $R$ factor (working) (%)/no. of reflections | 17.2/126448 | 16.5/128340 |
| $R$ factor (free) (%)/no. of reflections | 19.7/6674 | 19.1/6793 |
| no. of protein atoms | 7180 | 7184 |
| no. of heteroatoms | 774[b] | 954[c] |
| average $B$ value (Å$^2$) | | |
| protein atoms | 26.6 | 21.3 |
| ligand | 26.7 | 27.0 |
| solvent | 32.3 | 31.2 |
| weighted rmsd from ideality | | |
| bond lengths (Å) | 0.012 | 0.011 |
| bond angles (deg) | 2.5 | 2.2 |
| planar groups (Å) | 0.011 | 0.009 |
| Ramachandran regions (%)[d] | | |
| most favored | 90.1 | 91.0 |
| additionally allowed | 8.8 | 7.9 |
| generously allowed | 0.3 | 0.3 |
| disallowed | 0.8 | 0.8 |

[a] $R$ factor = $(\sum|F_o - F_c|/\sum|F_o|) \times 100$, where $F_o$ is the observed structure factor amplitude and $F_c$ is the calculated structure factor amplitude. [b] These include two dTDP-D-fucose molecules, two dTDP-L-rhamnose molecules, and 634 waters. [c] These include two dTDP-benzene molecules, two dTDP-L-rhamnose molecules, six ethylene glycol molecules, and 798 waters. [d] Distribution of Ramachandran angles according to PROCHECK.[34]

**Activity Assays.** As shown in Scheme 1, the substrate for EvaA is dTDP-4-keto-6-deoxyglucose. This ligand is not commercially available, and thus, it was necessary to prepare it enzymatically as previously described.[24,25] In addition, the product of EvaA is a diketo sugar, which is inherently unstable and as such cannot be detected by high-performance liquid chromatography. Thus, to measure the activity of EvaA, an in situ coupled assay was developed as outlined in Scheme 2. By utilizing the enzymes outlined in Scheme 2, it was possible to measure the activity of EvaA by monitoring the decrease in absorbance at 340 nm as NADPH is oxidized to $NADP^+$ due to the action of KijD10. Note that previous studies from our laboratory have verified that KijD10 from *Actinomadura kijaniata* functions as an NADPH-dependent C-3′-ketoreductase.[26] For these assays, reaction mixtures contained 50 mM HEPES (pH 7.5), 0.5 mM dTDP-glucose, 200 μM NADPH, 1 mg/mL 4,6-dehydratase (RmlB from *E. coli*), 0.002 mg/mL 2,3-dehydratase (EvaA), and 1 mg/mL 3-ketoreductase (KijD10). The required 4,6-dehydratase (RmlB) was cloned and purified in the laboratory (unpublished results). The reactions were initiated via the addition of EvaA and were conducted at 25 °C on a Beckman Coulter DU-640

**Scheme 2. Pathway Used To Monitor EvaA Activity**

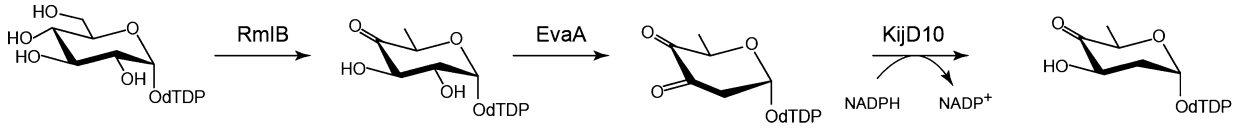


**Scheme 3. Enzymatic Synthesis of dTDP-Fucose**

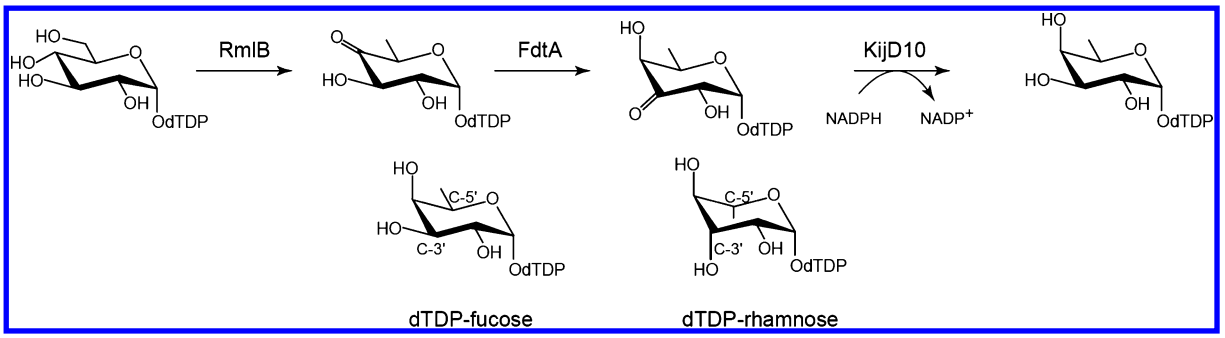


spectrophotometer (Beckman Coulter) for 5 min. Control reactions conducted in the absence of any one of the enzymes (RmlB, EvaA, or KijD10) resulted in no decrease in absorbance, thereby indicating that neither NADPH oxidation nor sugar reduction occurred. These control experiments demonstrated that both wild-type EvaA and the R381A mutant enzyme are, indeed, active and that NADPH is oxidized only in the presence of KijD10 and its proper dTDP-linked sugar substrate.

**Determination of Kinetic Constants.** Steady-state kinetic parameters for the wild type and the R381A mutant version of EvaA were determined via the spectrophotometric assay described above. All reaction mixtures contained 50 mM HEPES (pH 7.5), 200 $\mu$M NADPH, 2 mg/mL RmlB, 1 mg/mL KijD10, and dTDP-glucose concentrations ranging from 0.01 to 8 mM. These reactions were run using 2.0 $\mu$g/mL wild-type EvaA or the R381A mutant enzyme. Buffer, dTDP-glucose, and RmlB were mixed and incubated at 25 °C for 5 min to allow the accumulation of the EvaA substrate. NADPH and KijD10 were subsequently added to the mixture. The reaction was then initiated via the addition of EvaA and monitored at 25 °C on a Beckman Coulter DU-640 spectrophotometer (Beckman Coulter) for 5 min. Reduction of the 3,4-diketosugar substrate by KijD10 with the concurrent oxidation of NADPH to $NADP^+$ was followed by a decrease in absorbance at 340 nm. Slight substrate inhibition was seen at dTDP-glucose concentrations of >2 mM. Thus, the data were fit to the substrate inhibition equation $v_0 = (V_{max}[S])/[K_M + [S](1 + [S]/K_i)]$, where $K_i$ is the dissociation constant for substrate binding that takes into account the fact that two different substrates can bind to the enzyme. The $k_{cat}$ values were calculated according to the equation $k_{cat} = V_{max}/[E_T]$, where $E_T$ assumes one active site per EvaA subunit.

**Preparation and Analysis of Site-Directed Mutant Proteins.** To test the roles of Glu 139, Glu 190, Asp 353, Glu 404, Glu 405, and Glu 452 in the activity of EvaA, nine site-directed mutant proteins were constructed: E139Q, E190Q, E190A, D353A, E404Q, E405Q, E405A, E452Q, and E452A. The mutations were introduced into the EvaA R381A mutant protein via methods identical or similar to those described within the QuikChange site-directed mutagenesis kit. All primers required for the site-directed mutagenesis experiments are listed in Table S1 of the Supporting Information. Each mutant protein was expressed and purified, and the His tag was removed in a manner identical to that previously described for the wild-type enzyme except that the mutant proteins were dialyzed against 10 mM Tris (pH 8.0) and 200 mM NaCl and concentrated to 7−10 mg/mL.

The activities of these site-directed mutant proteins were studied via the spectrophotometric assay described above. For these tests, reaction mixtures contained 50 mM HEPES (pH 7.5), 0.5 mM dTDP-glucose, 200 $\mu$M NADPH, 1 mg/mL 4,6-dehydratase (RmlB), 0.02−2.0 mg/mL 2,3-dehydratase (EvaA), and 1 mg/mL 3-ketoreductase (KijD10).

**Production of dTDP-Fucose.** The enzymatic synthesis of dTDP-fucose required for the structural studies described here was accomplished via the pathway shown in Scheme 3. Previous studies from our laboratory have verified that FdtA from *Aneurinibacillus thermoaerophilus* functions as a 3,4-ketoisomerase.[27] By utilizing the enzymes outlined in Scheme 3, dTDP-fucose was produced on a large scale as follows. Each reaction mixture contained 12 mM dTDP-glucose, 50 mM HEPES (pH 7.5), 15 mM NADPH (Sigma), 0.5 mg/mL RmlB, 0.5 mg/mL FdtA, and 0.5 mg/mL KijD10. The reaction mixtures were incubated at 25 °C overnight, after which they were passed through a 10 kDa cutoff filter (Amicon) to remove the enzymes. The filtrates were then diluted 1:9 with water. Contaminants were removed from the reaction flow-through using an ÄKTA Purifier high-performance liquid chromatography system (GE Healthcare) equipped with a Resource-Q 6 mL anion exchange column (GE Healthcare). The column was first equilibrated with water, after which the reaction flow-through was loaded onto it. The column was then washed and eluted with a linear gradient to 50% 2 M ammonium acetate (pH 4.0) over 15 column volumes. The flow rate was 6 mL/min, and the elution was monitored at 267 nm.

The identity of dTDP-fucose was confirmed by ESI mass spectrometry (Mass Spectrometry/Proteomics Facility at the University of Wisconsin) and NMR spectroscopy (Nuclear Magnetic Resonance Facility, University of Wisconsin). The ESI mass spectrometry parent ion for dTDP-fucose was at $m/z$ 547.1. The observed NMR values were in agreement with those previously determined for dTDP-fucose.[28]


dx.doi.org/10.1021/bi400176n | *Biochemistry* 2013, 52, 2078−2088

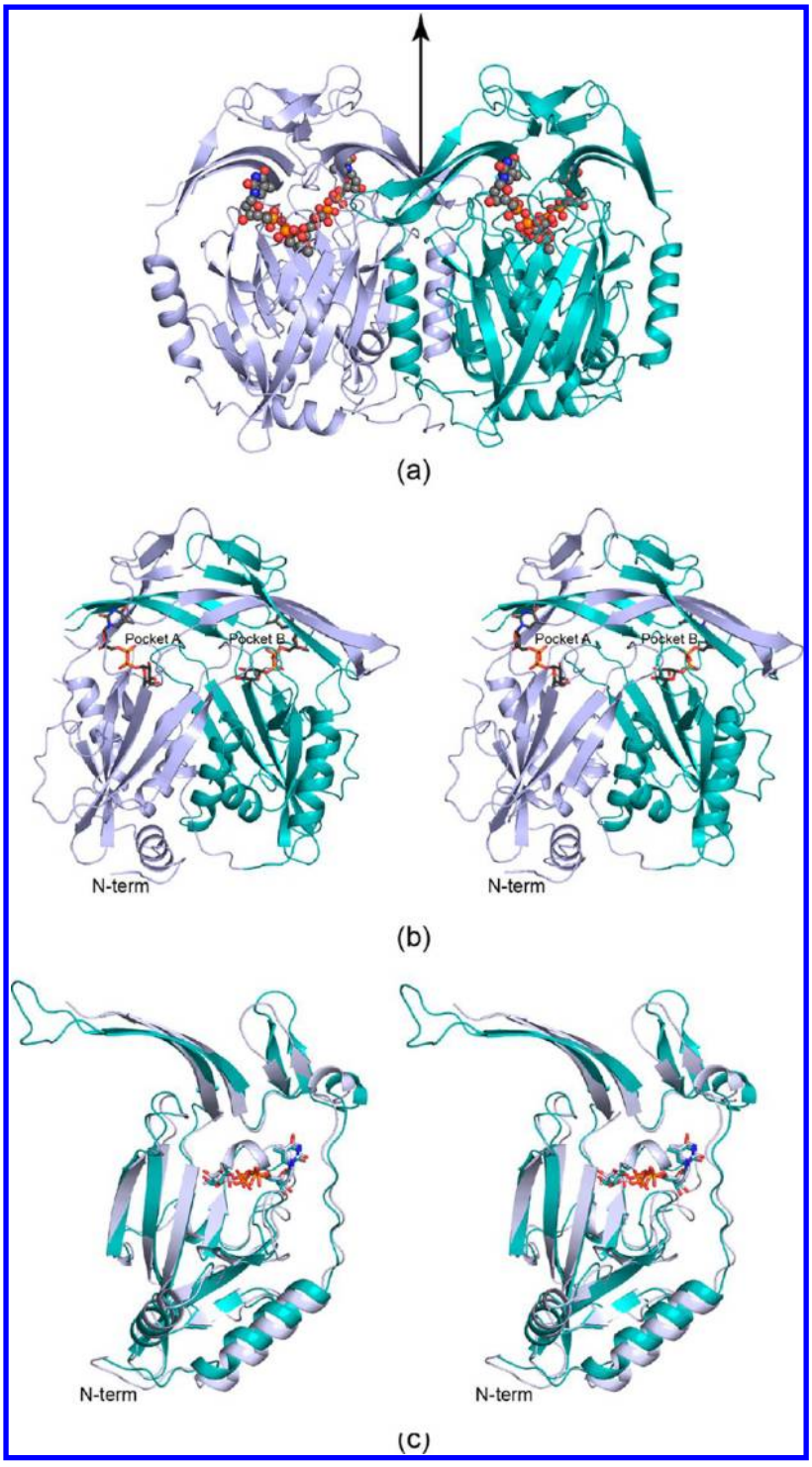


**Figure 1.** Structure of EvaA. A ribbon representation of the dimer is shown in panel a. The 2-fold rotational axis of the dimer, indicated by the black arrow, is coincident to a crystallographic dyad. An individual subunit is displayed as a stereoview in panel b. The EvaA subunit can be envisioned in terms of two domains, colored light blue and teal. The bound ligands are shown as sticks. As can be seen in panel c, the overall folds of the two domains are nearly identical to one another. The domains show amino acid sequence identities and similarities of 25 and 63%, respectively. All figures were prepared with PyMOL.[35]

## RESULTS AND DISCUSSION

**Overall Structure of EvaA.** Nearly 10 years ago, we initiated a structural investigation of TylX3 from *S. fradiae*. It was never possible to express soluble protein let alone grow diffraction-quality crystals to support a high-resolution X-ray analysis. After many attempts with seven additional homologous proteins, we were finally able to clone, overexpress, and purify EvaA from *A. orientalis*. The initial crystals of the enzyme belonged to space group $P2_1$ with four subunits in the asymmetric unit. They diffracted to, at best, 3.5 Å resolution. Utilizing crystals of a selenomethionine-labeled protein and X-ray data collected at Argonne National Laboratory, a preliminary electron density map for EvaA, in complex with

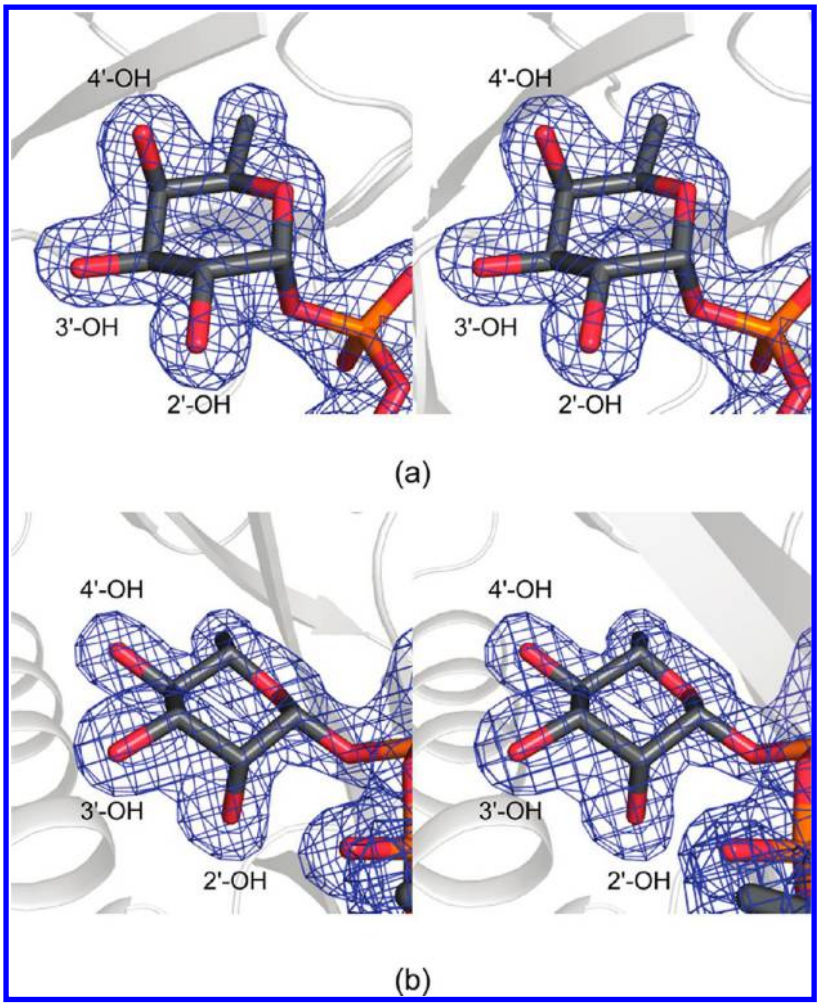


**Figure 2.** Representative electron density. Shown in panel a is the electron density corresponding to the pyranosyl moiety of the dTDP-sugar ligand bound to pocket A. The electron density is unambiguous for fucose. The electron density corresponding to the pyranosyl moiety of the dTDP-sugar ligand bound to pocket B is also unambiguous and shows the presence of rhamnose. Both maps were calculated with coefficients of the form $F_o - F_c$, where $F_o$ was the native structure factor amplitude and $F_c$ was the calculated structure factor amplitude. Each map was contoured at $2\sigma$.

dTDP-fucose, was obtained approximately a year ago via MAD phasing. The map was of sufficient quality to trace approximately two-thirds of the molecule. The electron densities for many of the side chains were not well-defined, however, and there were clearly ambiguities in the chain tracing.

A two-pronged approach was subsequently taken to improve the quality of the crystals. The first was to employ the concept of surface entropy reduction.[19,20] Accordingly, three protein variants were constructed (E231A/E233A, K289A/Q290A/E293A, and E316A/K317A), and all were subjected to crystallization trials. None of the resulting crystals demonstrated improved diffraction properties. The second approach was to consider the crystalline contacts in the $P2_1$ lattice and to modify surface residues with the goal of reducing the number of subunits in the asymmetric unit. For this approach, four mutant proteins were constructed and purified: R381A, D386A, S394A, and D127A. With the exception of the R381A mutant protein, none of the others displayed improved crystallization parameters. The R381A mutant protein, however, crystallized in the space group $P2_12_12$ with two monomers in the asymmetric unit. Excitingly, the crystals diffracted strongly to 1.7 Å resolution.

To ensure that the R381A mutant protein used in this investigation was catalytically active, experiments were conducted via an in situ coupled assayed as outlined in Scheme 2. This assay follows spectrophotometrically the formation of $NADP^+$ upon reduction of the diketosugar product resulting from the action of EvaA. The mutation had little effect on the overall catalytic efficiency of the enzyme. Specifically the $K_m$ and $V_{max}$ values for the wild type enzyme were $0.056 \pm 0.007$ mM and $(1.0 \pm 0.02) \times 10^{-4}$ mM $min^{-1}$, respectively. For the R381A mutant protein, the $K_m$ and $V_{max}$ values were $0.038 \pm 0.004$ mM and $(9.9 \pm 0.2) \times 10^{-3}$ mM $min^{-1}$, respectively. In light of these values and for the sake of simplicity, the R381A variant will hereafter be referred to as EvaA.

The crystals of EvaA contained two subunits in the asymmetric unit that were unrelated by a 2-fold rotational axis. To determine the oligomerization state of EvaA, ultracentrifugation experiments were conducted and clearly revealed the presence of dimers (Figure S1 of the Supporting Information). Thus, in the EvaA crystalline lattice, the dimers packed with their local dyads coincident to crystallographic 2-fold axes.

Each subunit is composed of 471 amino acid residues. The polypeptide chain backbones for both subunits were continuous and well-defined from Ala 11 to Arg 468, with the


dx.doi.org/10.1021/bi400176n | *Biochemistry* 2013, 52, 2078−2088

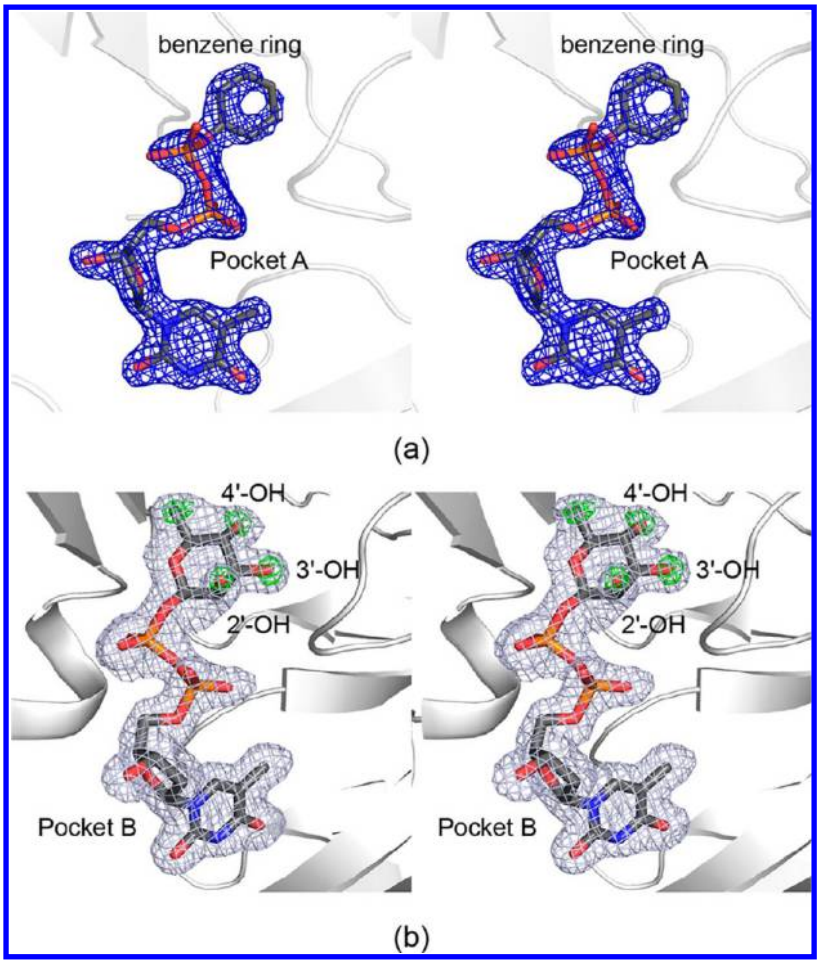


**Figure 3.** Electron density for the ligands following soaking experiments. Shown in panel a is the electron density observed in pocket A after the crystals were soaked in dTDP-benzene. The map was contoured at 2$\sigma$ and calculated with $F_o - F_c$ coefficients as described in the legend of Figure 2. The electron density observed in pocket B is displayed in panel b. The light blue-colored mesh corresponds to the electron density map calculated with coefficients of the form $2F_o - F_c$, and assuming that dTDP-benzene was bound. The map was contoured at 1$\sigma$. Superimposed on the blue mesh is an electron density map (green) calculated with $F_o - F_c$ coefficients and contoured at 4$\sigma$. Clearly dTDP-benzene was not bound in pocket B but dTDP-rhamnose was, indicating that this ligand is not easily exchanged in the crystalline lattice.

exceptions of two short breaks in each subunit (between Thr 160−Asn 167 and Ser 313−Ala 381 in subunit 1 and between Tyr 159−Asn 167 and Gly 312−Ile 318 in subunit 2) . The only significant outliers in the Ramachandran plot were Phe 83, Leu 145, Tyr 302, and Thr 359 in each subunit. The electron density was unambiguous for these residues, however. Both Phe 83 and Tyr 302 form stacking interactions with the thymine bases of the dTDP-sugar ligands as discussed further below.

Shown in Figure 1a is a ribbon representation of the EvaA dimer. The molecule has overall dimensions of approximately 70 Å × 90 Å × 60 Å. The subunit−subunit interface is extensive with a total buried surface area of 5000 Å$^2$. A close-up view of one subunit is provided in Figure 1b. The main body of the subunit displays an almost bowl-shaped appearance with the exterior formed by two mixed $\beta$-sheets and three $\alpha$-helices. Contained within the bowl are four $\alpha$-helical regions. The bowl is covered on the top by layers of antiparallel $\beta$-strands. Within each monomer there are two binding pockets, A and B, for the dTDP-sugar ligands as indicated by the stick representations in Figure 1b. These binding pockets are exposed to the solvent in the crystalline lattice. Both Pro 102 and Pro 176 adopt *cis* conformations. Pro 102 resides near the opening of pocket B, whereas Pro 176 is situated on the surface ~18 Å from pocket A. The regions, defined by Ala 29−Thr 234 and Asp 250−Glu 405, are related by a rotation of 179.6°. Indeed, the $\alpha$-carbons for these regions superimpose with an rmsd of 1.4 Å (Figure 1c), suggesting that the present day version of EvaA arose via gene duplication.

It was previously suggested in the literature that EvaA requires zinc for activity.[7,8] The high-resolution electron density maps utilized in this investigation did not reveal the presence of any zinc ions, and there are no apparent zinc binding sites in either domain of the EvaA subunit.

**Active Site Architecture of EvaA.** The dTDP-fucose used in this investigation was prepared enzymatically as outlined in Scheme 3. Shown in panels a and b of Figure 2 are the observed electron densities corresponding to the bound ligands in pockets A and B, respectively. As can be seen, the electron density in pocket A clearly reveals the presence of dTDP-fucose. Surprisingly, the electron density in pocket B shows that dTDP-rhamnose, rather than dTDP-fucose, is bound. The differences between fucose and rhamnose arise from the stereochemistries about the C-3′ and C-5′ positions (Scheme 3). Given the manner in which the dTDP-fucose was enzymatically synthesized, the obvious question is how dTDP-rhamnose arose as a contaminant. There are two


dx.doi.org/10.1021/bi400176n | *Biochemistry* 2013, 52, 2078−2088

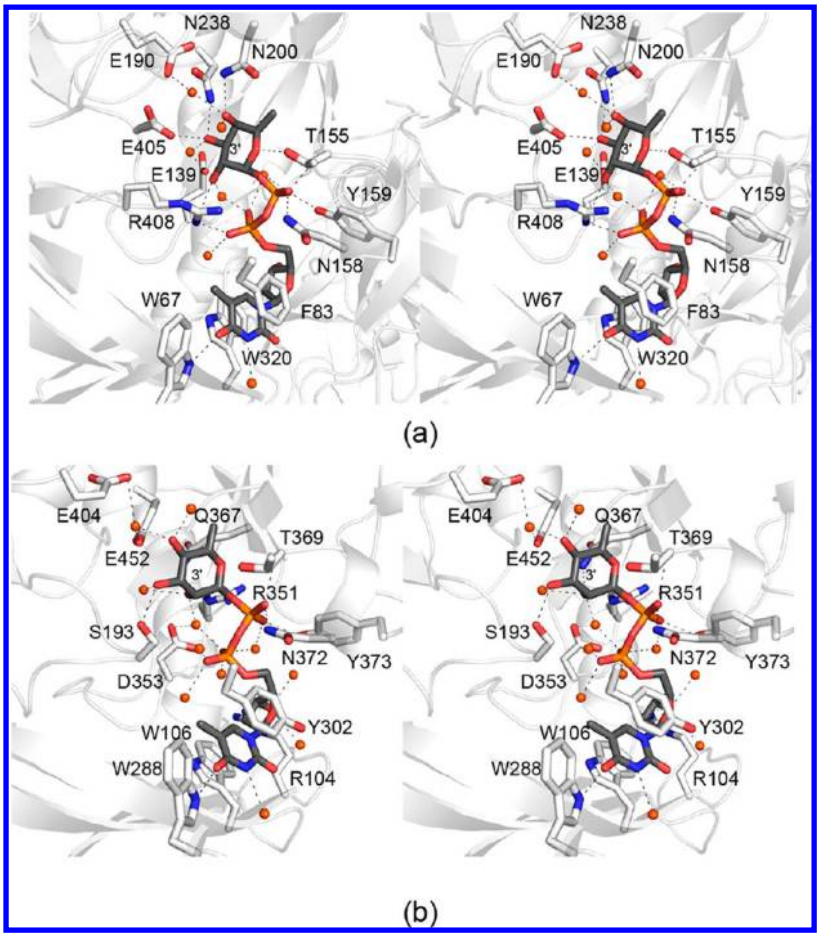


**Figure 4.** Close-up views of pockets A and B. Those residues lying within approximately 3.2 Å of dTDP-fucose and dTDP-rhamnose are displayed in panels a and b, respectively. The dTDP-sugars are highlighted with filled gray bonds. Water molecules are depicted as red spheres. The dashed lines indicate potential hydrogen bonds.

**Scheme 4. Proposed Catalytic Mechanism for Sugar 2,3-Dehydratases**

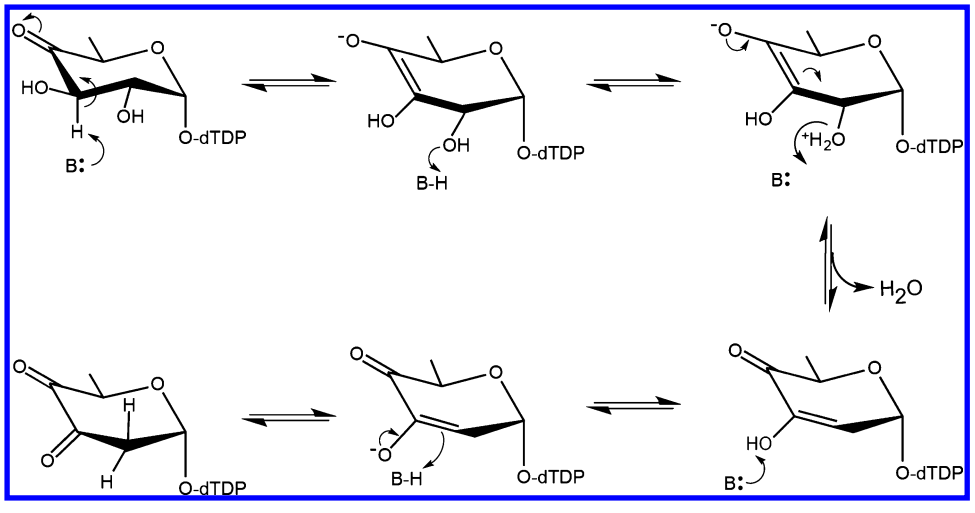


possible explanations. The first is that nonenzymatic epimerization occurred around the C-5′ position of dTDP-4-keto-6-deoxyglucose, which is the product of the RmlB reaction (Scheme 3). Isomerization then occurred via the reaction catalyzed by FdtA, and KijD10 subsequently reduced the C-3′ keto moiety to yield an axially rather than equatorially disposed hydroxyl group. This hypothesis assumes that FdtA functions on a substrate with altered stereochemistry about the C-5′ position, and because of the change in stereochemistry about the C-5′ atom, the dTDP-sugar product generated by FdtA binds in the KijD10 active site in a different orientation resulting in an axially disposed hydroxyl group. Alternatively, it is possible that FdtA is a promiscuous enzyme that not only displays isomerase activity but also can function as a C-5′ epimerase. Indeed, FdtA belongs to the "cupin" superfamily in which some members function as C-5′ epimerases.[29] These


dx.doi.org/10.1021/bi400176n | *Biochemistry* 2013, 52, 2078−2088

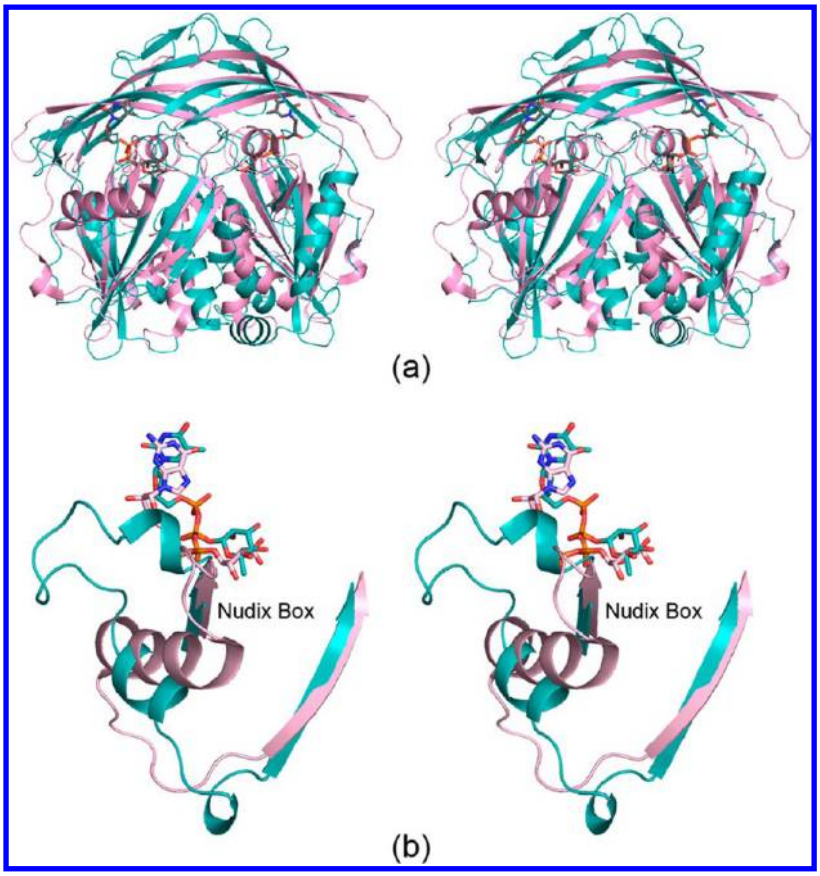


**Figure 5.** EvaA belongs to the Nudix superfamily. Shown in panel a is a superposition of the EvaA monomer (teal) onto the GDP-mannose hydrolase dimer (pink). Coordinates for GDP-mannose hydrolase were determined by the Amzel laboratory and obtained from the Protein Data Bank (entry 3O61).[31] Until this study, Nudix superfamily members were identified by a characteristic signature sequence of 23 amino acids that are located in a loop−helix−loop motif. This motif in GDP-mannose hydrolase is colored light pink in panel b. Superimposed upon it is the same region in EvaA, which does not contain the conserved "Nudix box". As shown, the two $\beta$-strands in each protein are connected by a different topological arrangement.

enzymes require both a tyrosine and a histidine residue for activity, which in FdtA adopt the same spatial positions. Experiments are underway to test these hypotheses. Regardless, the structural data clearly reveal that pocket A accepts dTDP-fucose, which serves as a mimic of the natural substrate for EvaA. Pocket B, on the other hand, selects for dTDP-rhamnose.

To test whether both pockets can exchange dTDP-sugar ligands, crystals grown in the presence of dTDP-fucose (with dTDP-rhamnose as a contaminant) were subsequently soaked in a synthetic mother liquor containing dTDP-benzene. An X-ray data set was collected, and the structure was determined to 1.7 Å resolution. Shown in panels a and b of Figure 3 are the electron densities corresponding to the ligands observed binding in pockets A and B, respectively. Clearly, dTDP-benzene exchanged for dTDP-fucose in pocket A, whereas in pocket B, dTDP-rhamnose remained bound.

Close-up views of the binding pockets for dTDP-fucose and dTDP-rhamnose are displayed in panels a and b of Figure 4, respectively. In both cases, the thymine rings of the ligands are sandwiched between aromatic groups (Phe 83 and Trp 320 in pocket A and Trp 106 and Tyr 302 in pocket B). Likewise, Trp 67 and Trp 288, in pockets A and B, respectively, lie within hydrogen bonding distance of a thymine carbonyl oxygen. Both pockets contain a tyrosine residue (Tyr 159 and Tyr 373) that is located within 3.2 Å of a phosphoryl oxygen. The largest differences between the two ligand-binding regions arise around the hexose moieties. In pocket A, the fucose group is positioned within hydrogen bonding distance of five side chains (Thr 155, Asn 200, Asn 238, Asp 405, and Arg 408), whereas in pocket B, the rhamnose directly interacts with only two side chains (Ser 193 and Gln 367).

**Analysis of Site-Directed Mutant Proteins.** A possible catalytic mechanism for sugar 2,3-dehydratases, as outlined in Scheme 4, was proposed more than 10 years ago.[8] In this mechanism, an active site base is thought to abstract the proton attached to C-3′ of the hexose, leading to the formation of an enolate intermediate. The proton is delivered to the C-2′ hydroxyl, which departs as a water molecule. The catalytic base then abstracts a proton from the C-3′ hydroxyl and delivers it to C-2′.

In the structures of EvaA presented here, there are no apparent side chains in the proper position in either binding pocket to serve in such a capacity. However, it must be kept in mind that the dTDP-sugars used in this investigation are substrate analogues. The true substrate for EvaA contains a keto group at the C-4′ position, and thus, the hexose group in the substrate analogue may be adopting a conformation that does not mimic the true substrate. With this in mind, six side chains that could possibly function as active site bases were targeted for study. Three are located in pocket A (Glu 139, Glu 190, and Glu 405), and three are found in pocket B (Asp 353, Glu 404, and Glu 452). Their positions can be seen in panels a and b of

Figure 4. None is located within 3.5 Å of the hexose C-3′ atom, however. In addition, the only amino acid residue that lies in the proper position to abstract a hydrogen from the hexose C-3′ atom is Glu 139, but it is situated 4.8 Å from the hexose C-3′ atom.

Activity assays conducted on the E139Q, E190Q, E190A, E405Q, and E405A mutant proteins demonstrated complete loss of enzymatic activities (Figure S2 of the Supporting Information). Importantly, all of these residues are strictly conserved among the 2,3-dehydratases (Figure S3 of the Supporting Information). Activity assays on the D353A and E452Q forms of EvaA revealed that these proteins retained their catalytic activity (Figure S2 of the Supporting Information). The E452A and E404Q proteins were enzymatically inactive. These glutamate residues reside in a region between pockets A and B. Most likely, mutation of these residues resulted in structural perturbations that propagated to pocket A. Whereas Glu 404 is completely conserved among the 2,3-dehydratases, Glu 452 is not. Taken together, these studies strongly suggest that the EvaA active site is confined within pocket A.

**EvaA and the Nudix Hydrolase Superfamily.** A search of the Protein Data Bank using secondary structure matching (SSM) revealed that the fold of the EvaA subunit closely matches the dimeric architecture of GDP-mannose hydrolase from *E. coli*, which belongs to the Nudix hydrolase superfamily (Figure 5a).[30,31] Members of this large and mechanistically diverse superfamily typically require $Mg^{2+}$ for activity and catalyze the hydrolysis of a wide range of organic pyrophosphates.[13,14,32] They are found throughout the biological kingdom, from viruses and bacteria to eukaryotes, and they are thought to serve in protective, regulatory, and signaling roles. In mechanistic terms, most family members catalyze nucleophilic substitutions at phosphorus atoms. Most are characterized by a conserved 23-residue sequence $GX_5EX_7R$-EUXEEXGU motif, where U corresponds to a hydrophobic residue and X is any residue. The Nudix motif provides both catalytic and $Mg^{2+}$ binding residues. EvaA is a highly unusual member of this superfamily in that it does not contain the characteristic sequence motif, does not bind or require $Mg^{2+}$ for activity, and does not catalyze a hydrolysis reaction but rather a 2,3-dehydration. Indeed, it is in the Nudix signature sequence region where EvaA and GDP-mannose hydrolase diverge significantly (Figure 5b).

Thus far, 29400 amino acid sequences have been identified as belonging to the Nudix hydrolase superfamily according to the Sanger Institute's Pfam database. None of these sequences encode a 2,3-dehydratase, however. From our investigation, it is now clear that many more family members will be identified as search algorithms are expanded to include the sequences of EvaA and other 2,3-dehydratases.[33]

## ■ ASSOCIATED CONTENT

### Supporting Information

All primers used in this study, ultracentrifugation data, enzyme activity assay plots, and amino acid sequence alignments of 2,3-dehydratase homologues (Table S1 and Figures S1−S3, respectively). This material is available free of charge via the Internet at http://pubs.acs.org.

### Accession Codes

X-ray coordinates have been deposited in the Protein Data Bank as entries 4J7G and 4J7H.

## ■ AUTHOR INFORMATION


### Corresponding Author

*E-mail: hazel_holden@biochem.wisc.edu. Fax: (608) 262-1319. Phone: (608) 262-4988.



### Funding

This research was supported in part by National Science Foundation (NSF) Grant MCB-0849274 to H.M.H. and NSF Predoctoral Fellowship DGE-0718123 to R.L.K.


### Notes

The authors declare no competing financial interest.

## ■ ACKNOWLEDGMENTS


We thank Professors Grover L. Waldrop, Vahe Bandarian, and George Reed for helpful comments. A portion of the research described in this paper was performed at the Structural Biology Center of the Advanced Photon Source of Argonne National Laboratory (U.S. Department of Energy, Office of Biological and Environmental Research, under Contract DE-AC02-06CH11357). We gratefully acknowledge Dr. Norma E. C. Duke for assistance during the X-ray data collection at Argonne National Laboratory.


## ■ ABBREVIATIONS

DTT, dithiothreitol; ESI, electrospray ionization; HEPES, *N*-(2-hydroxyethyl)piperazine-*N*′-2-ethanesulfonic acid; MES, 2-(*N*-morpholino)ethanesulfonic acid; NMR, nuclear magnetic resonance; rmsd, root-mean-square deviation; TEV, tobacco etch virus; Tris, tris(hydroxymethyl)aminomethane.

## ■ REFERENCES


(1) Thibodeaux, C. J., Melancon, C. E., and Liu, H. W. (2007) Unusual sugar biosynthesis and natural product glycodiversification. *Nature 446*, 1008−1016.

(2) Thibodeaux, C. J., Melancon, C. E., III, and Liu, H. W. (2008) Natural-product sugar biosynthesis and enzymatic glycodiversification. *Angew. Chem., Int. Ed. 47*, 9814−9859.

(3) Hunt, A. H., Molloy, R. M., Debono, M., and Occolowitz, J. L. (1988) Isolation and characterization of 4-*epi*-vancosamine. *Tetrahedron Lett. 29*, 1223−1226.

(4) Moeck, G. (2008) Oritavancin: The discovery and development of a novel lipoglycopeptide antibiotic. *AMRI Technical Reports*,.

(5) Weymouth-Wilson, A. C. (1997) The role of carbohydrates in biologically active natural products. *Nat. Prod. Rep. 14*, 99−110.

(6) Chen, H., Thomas, M. G., Hubbard, B. K., Losey, H. C., Walsh, C. T., and Burkart, M. D. (2000) Deoxysugars in glycopeptide antibiotics: Enzymatic synthesis of TDP-L-epivancosamine in chloroeremomycin biosynthesis. *Proc. Natl. Acad. Sci. U.S.A. 97*, 11942−11947.

(7) Chen, H., Agnihotri, G., Guo, Z., Que, N. L. S., Chen, X. H., and Liu, H.-w. (1999) Biosynthesis of mycarose: Isolation and characterization of enzymes involved in the C-2 deoxygenation. *J. Am. Chem. Soc. 121*, 8124−8125.

(8) He, X. M., and Liu, H. W. (2002) Formation of unusual sugars: mechanistic studies and biosynthetic applications. *Annu. Rev. Biochem. 71*, 701−754.

(9) Gaisser, S., Bohm, G. A., Doumith, M., Raynal, M. C., Dhillon, N., Cortes, J., and Leadlay, P. F. (1998) Analysis of eryBI, eryBIII and eryBVII from the erythromycin biosynthetic gene cluster in *Saccharopolyspora erythraea*. *Mol. Gen. Genet. 258*, 78−88.

(10) Westrich, L., Domann, S., Faust, B., Bedford, D., Hopwood, D. A., and Bechthold, A. (1999) Cloning and characterization of a gene cluster from *Streptomyces cyanogenus* S136 probably involved in landomycin biosynthesis. *FEMS Microbiol. Lett. 170*, 381−387.

(11) Torkkell, S., Ylihonko, K., Hakala, J., Skurnik, M., and Mantsala, P. (1997) Characterization of *Streptomyces nogalater* genes encoding

enzymes involved in glycosylation steps in nogalamycin biosynthesis. *Mol. Gen. Genet. 256*, 203−209.
(12) Ichinose, K., Bedford, D. J., Tornus, D., Bechthold, A., Bibb, M. J., Revill, W. P., Floss, H. G., and Hopwood, D. A. (1998) The granaticin biosynthetic gene cluster of *Streptomyces violaceoruber* Tu22: Sequence analysis and expression in a heterologous host. *Chem. Biol. 5*, 647−659.
(13) Mildvan, A. S., Xia, Z., Azurmendi, H. F., Saraswat, V., Legler, P. M., Massiah, M. A., Gabelli, S. B., Bianchet, M. A., Kang, L. W., and Amzel, L. M. (2005) Structures and mechanisms of Nudix hydrolases. *Arch. Biochem. Biophys. 433*, 129−143.
(14) McLennan, A. G. (2006) The Nudix hydrolase superfamily. *Cell. Mol. Life Sci. 63*, 123−143.
(15) Thoden, J. B., Timson, D. J., Reece, R. J., and Holden, H. M. (2005) Molecular structure of human galactokinase: Implications for Type II galactosemia. *J. Biol. Chem. 280*, 9662−9670.
(16) Otwinowski, Z., and Minor, W. (1997) Processing of X-ray diffraction data collected in oscillation mode. *Methods Enzymol. 276*, 307−326.
(17) Terwilliger, T. C., and Berendzen, J. (1999) Automated MAD and MIR structure solution. *Acta Crystallogr. D55* (Part 4), 849−861.
(18) Emsley, P., and Cowtan, K. (2004) Coot: Model-building tools for molecular graphics. *Acta Crystallogr. D60*, 2126−2132.
(19) Derewenda, Z. S. (2004) Rational protein crystallization by mutational surface engineering. *Structure 12*, 529−535.
(20) Goldschmidt, L., Cooper, D. R., Derewenda, Z. S., and Eisenberg, D. (2007) Toward rational protein crystallization: A Web server for the design of crystallizable protein variants. *Protein Sci. 16*, 1569−1576.
(21) McCoy, A. J., Grosse-Kunstleve, R. W., Adams, P. D., Winn, M. D., Storoni, L. C., and Read, R. J. (2007) Phaser crystallographic software. *J. Appl. Crystallogr. 40*, 658−674.
(22) Cowtan, K. (1994) 'DM:' An automated procedure for phase improvement by density modification. *Joint CCP4 and ESF-EACBM Newsletter on Protein Crystallography 31*, 34−38.
(23) Murshudov, G. N., Vagin, A. A., and Dodson, E. J. (1997) Refinement of macromolecular structures by the maximum-likelihood method. *Acta Crystallogr. D53*, 240−255.
(24) Hong, L., Zhao, Z., Melancon, C. E., III, Zhang, H., and Liu, H. W. (2008) *In vitro* characterization of the enzymes involved in TDP-D-forosamine biosynthesis in the spinosyn pathway of *Saccharopolyspora spinosa*. *J. Am. Chem. Soc. 130*, 4954−4967.
(25) Thoden, J. B., Schaffer, C., Messner, P., and Holden, H. M. (2009) Structural analysis of QdtB, an aminotransferase required for the biosynthesis of dTDP-3-acetamido-3,6-dideoxy-α-D-glucose. *Biochemistry 48*, 1553−1561.
(26) Kubiak, R. L., and Holden, H. M. (2011) Combined structural and functional investigation of a C-3″-ketoreductase involved in the biosynthesis of dTDP-L-digitoxose. *Biochemistry 50*, 5905−5917.
(27) Davis, M. L., Thoden, J. B., and Holden, H. M. (2007) The X-ray structure of dTDP-4-keto-6-deoxy-D-glucose-3,4-ketoisomerase. *J. Biol. Chem. 282*, 19227−19236.
(28) Elling, L., Rupprath, C., Gunther, N., Romer, U., Verseck, S., Weingarten, P., Drager, G., Kirschning, A., and Piepersberg, W. (2005) An enzyme module system for the synthesis of dTDP-activated deoxysugars from dTMP and sucrose. *ChemBioChem 6*, 1423−1430.
(29) Field, R. A., and Naismith, J. H. (2003) Structural and mechanistic basis of bacterial sugar nucleotide-modifying enzymes. *Biochemistry 42*, 7637−7647.
(30) Krissinel, E., and Henrick, K. (2004) Secondary-structure matching (SSM), a new tool for fast protein structure alignment in three dimensions. *Acta Crystallogr. D60*, 2256−2268.
(31) Boto, A. N., Xu, W., Jakoncic, J., Pannuri, A., Romeo, T., Bessman, M. J., Gabelli, S. B., and Amzel, L. M. (2011) Structural studies of the Nudix GDP-mannose hydrolase from *E. coli* reveals a new motif for mannose recognition. *Proteins 79*, 2455−2466.
(32) Bessman, M. J., Frick, D. N., and O'Handley, S. F. (1996) The MutT proteins or "Nudix" hydrolases, a family of versatile, widely distributed, "housecleaning" enzymes. *J. Biol. Chem. 271*, 25059−25062.
(33) Finn, R. D., Mistry, J., Tate, J., Coggill, P., Heger, A., Pollington, J. E., Gavin, O. L., Gunasekaran, P., Ceric, G., Forslund, K., Holm, L., Sonnhammer, E. L., Eddy, S. R., and Bateman, A. (2010) The Pfam protein families database. *Nucleic Acids Res. 38*, D211−D222.
(34) Laskowski, R. A., Moss, D. S., and Thornton, J. M. (1993) Main-chain bond lengths and bond angles in protein structures. *J. Mol. Biol. 231*, 1049−1067.
(35) DeLano, W. L. (2002) *The PyMOL Molecular Graphics System*, DeLano Scientific, San Carlos, CA.